HHS Public Access

Author manuscript

Biomaterials. Author manuscript; available in PMC 2016 December 01.

Published in final edited form as:

Biomaterials. 2015 December ; 72: 1–10. doi:10.1016/j.biomaterials.2015.08.040.

Towards programming immune tolerance through geometric manipulation of phosphatidylserine

Reid A. Roberts[#a,c,2], **Timothy K. Eitas**[#a], **James D. Byrne**[#b,c], **Brandon M. Johnson**[a], **Patrick J. Short**[d], **Karen P. McKinnon**[a], **Shannon Reisdorf**[a], **J. Christopher Luft**[b], **Joseph M. DeSimone**[b,d,e,f,g,**], and **Jenny P. Ting**[a,h,i,j]

[a] Department of Microbiology and Immunology, University of North Carolina at Chapel Hill, Chapel Hill, NC 27599, USA

[b] Eshelman School of Pharmacy, Division of Molecular Pharmaceutics, University of North Carolina at Chapel Hill, Chapel Hill, NC 27599, USA

[c] School of Medicine, University of North Carolina at Chapel Hill, Chapel Hill, NC 27599, USA

[d] Department of Chemistry, University of North Carolina, Chapel Hill, NC 27599, USA

[e] Department of Pharmacology, University of North Carolina at Chapel Hill, Chapel Hill, NC 27599, USA

[f] Department of Chemical and Biomolecular Engineering, North Carolina State University, Raleigh, NC 27695, USA

[g] Sloan-Kettering Institute for Cancer Research, Memorial Sloan Kettering Comprehensive Cancer Center, New York, NY 10065, USA

[h] Center for Translational Immunology, University of North Carolina at Chapel Hill, Chapel Hill, NC 27599, USA

[i] Institute for Inflammatory Diseases, University of North Carolina at Chapel Hill, Chapel Hill, NC 27599, USA

[j] Department of Genetics, University of North Carolina at Chapel Hill, Chapel Hill, NC 27599, USA

[#] These authors contributed equally to this work.

Abstract

The possibility of engineering the immune system in a targeted fashion using biomaterials such as nanoparticles has made considerable headway in recent years. However, little is known as to how modulating the spatial presentation of a ligand augments downstream immune responses. In this report we show that geometric manipulation of phosphatidylserine (PS) through fabrication on rod-shaped PLGA nanoparticles robustly dampens inflammatory responses from innate immune

Correspondence to: Jenny P. Ting.

[**] Corresponding author. desimone@unc.edu (J.M. DeSimone)..

[2]Current address: Department of Emergency Medicine, Maine Medical Center, Portland, ME 04102, USA.

Appendix A. Supplementary data

Supplementary data related to this article can be found at http://dx.doi.org/10.1016/j.biomaterials.2015.08.040.

cells while promoting T regulatory cell abundance by impeding effector T cell expansion. This response depends on the geometry of PS presentation as both PS liposomes and 1 micron cylindrical PS-PLGA particles are less potent signal inducers than 80 × 320 nm rod-shaped PS-PLGA particles for an equivalent dose of PS. We show that this immune tolerizing effect can be co-opted for therapeutic benefit in a mouse model of multiple sclerosis and an assay of organ rejection using a mixed lymphocyte reaction with primary human immune cells. These data provide evidence that geometric manipulation of a ligand via biomaterials may enable more efficient and tunable programming of cellular signaling networks for therapeutic benefit in a variety of disease states, including autoimmunity and organ rejection, and thus should be an active area of further research.

Keywords

Autoimmunity; Immunoengineering; Immunomodulation; Nanoparticles; PRINT; PLGA; Phosphatidylserine; Tolerance; Transplantation

1. Introduction

Recent advances in multiple scientific fields, including materials science and immunology, are now converging to enable targeted, pathology-specific biological programming to promote health in living animals [1–4]. This is in part due to our increased understanding of the signaling pathways involved in a variety of disease states as well as our fundamental appreciation of the molecular interactions which underlie initiation and maintenance of immune responses. This information has been used to generate a new wave of therapeutic tools that program biological responses using rationally-designed biomaterials, including nanoparticles and hydrogels. Some examples of the programming potential of this new class of tools include more potent and sustained vaccine responses to pathogens [5–8], enhanced drug delivery and immunomodulation in the setting of cancer [9–18], amelioration of both acute and chronic inflammatory responses [19–22], and dampening autoimmunity and allergies through promotion of antigen-specific tolerance [23–25].

While the potential for nanotechnology to transform therapeutic approaches to the diseases that burden 21st century societies is readily apparent at this stage, there remain many unanswered mechanistic and design questions as relates to nanoparticle-mediated programming of biologic responses. In this report, we aimed to address one such fundamental question regarding the particulate presentation of a ligand that binds a cell surface receptor. This is a mechanistically critical question, as programming of biological responses will often require interface with cell surface receptors yet little is known as to how the geometric manipulation of ligands via biomaterials augments downstream biological signaling from the cell surface. Here, we use the term geometry to broadly define the three dimensional presentation of a ligand that can be manipulated through varying the size, shape, composition and biophysics of a particulate delivery vehicle. Given the recent finding that geometric manipulation of the erythropoietin cell surface receptor using diabodies can fundamentally alter downstream signaling effects, there is precedent for this concept [26].

To address this issue, we chose to use the cell membrane phospholipid phosphatidylserine (PS) as our model ligand for a cell surface receptor. PS is primarily localized on the inner membrane of cells until apoptosis triggers it to re-localize to the outer membrane where it can serve as an “eat-me” signal to phagocytes [27–29]. This is a critical means by which the body avoids aberrant immune response to self-antigens because the PS signal induces an anti-inflammatory program in the engulfing phagocyte which promotes tolerance to components of the dying cell. This is thought to be in part due to TGF-β1 release as well as triggering of cell surface receptors, including the PS receptor (PSR) and MERTK, a member of the TAM family of receptor tyrosine kinases [27,28], [30–32]. We hypothesized that particulate presentation of PS on a nanoparticle would mimic apoptotic cells and thus drive an anti-inflammatory program in innate immune cells. There is evidence for this using liposomal preparations of PS however we broadened our approach to specifically address how the geometry of PS presentation augmented its signaling effects and subsequent therapeutic potential [33–35]. In particular, we addressed how PS liposomes versus delivery of PS on 80 × 320 nm PLGA nanorods or 1 micron cylindrical PLGA particles affected downstream immune responses.

This latter feature of our paper – design control of particulate PS presentation – was made possible through using the Particle Replication in Non-Wetting Template (PRINT) process, which enables fabrication of particles of a homogenous size, shape, and charge composed of both lipids and polymers through a molding process [36–39]. We have previously shown that the PRINT process enables fabrication of nano- and microparticles made of poly lactic-co-glycolic acid (PLGA) or PEG (poly-ethylene glycol) that do not induce immune activation at baseline in mouse and human cells. We have also shown these particles can be designed to target mammalian innate immune cells *in vitro* and *in vivo* or remain extracellular, thus making them an attractive tool for programming immune responses for therapeutic benefit [40–43].

In this report we show that geometric manipulation of PS programs the immune response towards an anti-inflammatory state that dampens effector T cell expansion while promoting T regulatory cell abundance in a tunable fashion. We show that this anti-inflammatory response may possibly be co-opted for therapeutic benefit in a variety of disease states, including autoimmunity using a mouse model of multiple sclerosis and transplantation medicine approaches using a model of allogeneic human T cell activation. These results strongly suggest that particulate delivery of a cell surface receptor ligand can trigger unique signaling effects through geometric manipulation of the surface membrane. Therefore, geometric and biophysical properties of particles should be included as part of baseline experiments that seek to further the field of programming biological responses as it is highly likely each ligand of therapeutic interest will have its own unique ‘best-in-class’ particle design parameters.

2. Materials and methods

2.1. PRINT particle fabrication and characterization

For the incorporation of PS (Avanti Polar Lipids, 840032) in the PRINT platform, PS and poly(D,L-lactide-co-glycolide) (PLGA) of lactide:glycolide 85:15 (Sigma Aldrich) were

dissolved separately in chloroform. The solutions of PS and PLGA were mixed at ratios of 10:90 (PS:PLGA), and the sample was diluted to 2 wt% (mass/mass) solution with chloroform. A thin film of PS and PLGA was deposited on a 6″ × 12″ sheet of poly(ethylene terephthalate) (PET) by spreading 200 μL of solution using a #5 Mayer Rod (R.D. Specialties). The solvent was evaporated with heat. Fluorocur®, d = 80 nm × h = 320 nm, d = 1000 nm × h = 1000 nm prefabricated molds and 2000 g/mol polyvinyl alcohol (PVOH) coated PET sheets were provided by Liquidia Technologies. The PET sheet with the film was then placed in contact with the patterned side of a mold and passed through heated nips (Chem Instruments Hot Roll Laminator) at 130 °C and 80 psi. The mold was split from the PET sheet as they both passed through the hot laminator. The patterned side of the mold was then placed in contact with a sheet of PET sheet coated with 2000 g/mol PVOH. This was then passed through the hot laminator to transfer the particles from the mold to the PET sheet. The mold was then peeled from the PET sheet. The particles were removed by passing the PVOH coated PET sheet through motorized rollers and applying water to dissolve the PVOH to release the particles. To remove excess PVOH and unbound PS, the particles were purified and then concentrated by tangential flow filtration (Spectrum Labs). PS was resuspended in deionized, distilled water and did not undergo more than 1 freeze–thaw cycle during experimentation. The PLGA particles were imaged by scanning electron microscopy (SEM) by pipetting a 3 μL sample of particle on a glass slide. The sample was then dried and coated with 3 nm gold palladium alloy using a Cressington 108 auto sputter coater. Images were taken at an accelerating voltage of 2 kV using a Hitachi model S-4700 SEM. For size and zeta potential measurement, dynamic light scattering (DLS) (Malvern Instruments Nano-ZS) was used. The particles were suspended in 10 mM KCl solution for zeta potential measurements. PS was measured using an Agilent Technologies Series 1200 HPLC with a C18 reverse phase column (Zorbax Eclipse XDB-C18, 4.6 × 100 mm, 3.5 micron). A linear gradient from 85:15 of methanol with 0.1% trifluoroacetic acid (TFA): water with 0.1% TFA to 100% methanol with 0.1% TFA was run over 25 min at a flow rate of 1 ml/min. Particle samples were dissolved in an acetonitrile:water solution, and the PS was quantified using an ELSD detector. Liposomal PS formulations were generated through resuspension of unadulterated PS in sterile water.

2.2. Murine bone marrow-derived dendritic cell activation studies

Red blood cell-depleted bone marrow cells were harvested from the femurs and tibias of C57BL/6 mice as previously described [44]. These cells were cultured with 5 ng/ml GM-CSF in complete media (RPMI 1640 media containing 10 mM HEPES, 1 mM L-glutamine, 100 U/ml penicillin, 100 μg/ml streptomycin, 50 μM β-mercaptoethanol and 10% heat inactivated FBS) at 37 °C for 6 days and purified using anti-$CD11c^+$ beads (MACS). The six-day old bone marrow-derived dendritic cells (BMDCs) were incubated with PS-loaded PLGA nanoparticles (25 μM PS), PS alone (25 μM), or blank PLGA nanoparticles at 37 °C for 4 h, and the BMDCs were subsequently washed and stimulated with a Th1-like input (LPS/IFNγ). Eighteen hours post-stimulation, the BMDCs and media were separated for analysis. Cells were stained with an APC-labeled CD86 antibody (eBioscience, 17-0862-81) and the cell populations were quantified by flow cytometry analysis (CYAN Flow Cytometer). Mouse IL-6 (BD, 555240), mouse IL-12 p40 (BD, 555165), mouse PGE2

(Abcam, ab133055) ELISA sets were used for the analysis of the supernatant and were read using a fluorescence plate reader.

2.3. Myelin-specific murine T cell activation studies

Mouse T cells were purified from spleens of 2D2 mice, a genetically engineered mouse model with only T cells expressing T cell receptors to MOG, using anti-$CD4^+$ beads (MACS) [45]. Bone-marrow derived DCs were incubated with PS-loaded PLGA nanoparticles (12, 25, or 50 μM PS), PS alone (12, 25, or 50 μM), or blank PLGA nanoparticles at 37 °C for 4 h, and the cells were subsequently washed. For myelin-specific T cell activation, 5×10^4 DCs treated with PS-loaded PLGA nanoparticles, PS alone, or blank PLGA nanoparticles at 37 °C for 4 h were pulsed with $MOG_{35–55}$ peptide (50 μg/ml) and then incubated with 2×10^5 T cells for 48 h. The cells and media were separated, and the supernatant was probed for mouse IFNγ (Biolegend, 430806), mouse IL-2 (BD, 555148), mouse IL-6 (BD, 555240) mouse TNFα (BD, 555268). T-cells were stained with IL-10 (eBioscience, 12-7101) and FOXP3 (eBioscience, 17-5773-82) to identify the Treg population using flow cytometry.

2.4. EAE animal studies

All animal studies were performed with the approval of the UNC Institutional Animal Care and Use Committee (IACUC). EAE was performed as previously described [45,46]. Briefly, $MOG_{35–55}$ peptide (Genemed Synthesis Inc) was emulsified in complete Freund's adjuvant and mixed with heat-killed mycobacterium tuberculosis (4 mg/ml) using a luer-lock syringe system (Cadence, Inc). The emulsion was administered via subcutaneous injection to C57BL/6 mice on day 0. On day 7, which corresponded with the start of tail paralysis, PS alone (50 μg), PS-loaded 80 × 320 nm PLGA nanoparticles (50 μg PS), or an equivalent dose of blank 80 × 320 nm PLGA nanoparticles were administered via tail vein injection daily for 4 days. The following scale was used to assess clinical scores: 0 = Normal mouse, no overt sign of disease, 0.5 = Partial tail paralysis (loss of tip tail tonus), 1 = Limp tail or hind limb weakness but not both, 2 = Limb tail and hind limb weakness, 3 = Partial hind limb paralysis, 4 = Complete hind limb paralysis, 5 = Moribund state, sacrifice for humane reasons [46]. Results are indicative of a combination of two independent experiments.

2.5. Human mixed lymphocyte reaction studies

Blood was collected from healthy donors or leukapheresed patients in accordance with the University of North Carolina's Office of Human Research Ethics (IRB #12–1858 and #05–2860). Donors provided written informed consent and samples were anonymized and de-identified prior to use in the described studies. Peripheral blood mononuclear cells (PBMCs) were isolated from healthy donors using Ficoll Paque Premium (Fisher, 45-001-75). Dynabeads® Untouched™ Human CD4 T cells kit (Life Technologies, 11352D) were then used to isolate T cells. Allogenic T cell activation was performed by mixing 2×10^5 $CD4^+$ T cells from 2 donors with 5×10^4 DCs isolated from 1 donor. DCs were treated with PS-loaded PLGA nanoparticles (25 μM PS), PS alone (25 μM), or blank PLGA nanoparticles at 37 °C for 4 h prior to co-culture with T cells. The cells and media were separated after 7 days and the supernatant was probed for human IFNγ (BD, 555142). Human immune cell

flow analysis was performed with antibodies to either CD11c (eBio-science, 25-0116-42) or CD3 (eBioscience, 12-0037-42) on a CYAN Flow Cytometer.

2.6. Statistical analysis

All statistical comparisons were performed on GraphPad Prism (version 6.04). Two-tailed t-tests and ANOVA followed by Tukey post-hoc analysis were performed as indicated. A p-value of 0.05 or less was considered statistically significant.

3. Results

3.1. Fabrication and characterization of particles

We chose to fabricate 80 × 320 nm PLGA nanorods and 1 micron PLGA cylinders using the PRINT platform with and without encapsulated PS. We have previously published PRINT particles in this size range passively target both murine and human innate immune cells in a manner that does not significantly activate immune responses [40,41]. The PRINT process was used for fabrication of both 80 × 320 nm and 1 μm PS-loaded PLGA particles with a pre-particle solution composed of 10 wt% PS. The post-processed loading was determined to be 8 ± 2 wt% and 11 ± 3 wt% PS, respectively. As measured by dynamic light scattering, both PS-loaded PLGA nanorods and blank PLGA nanorods were ~210 nm in hydrodynamic diameter with PDI of less than or equal to 0.1. The PLGA cylinders had an average hydrodynamic diameter of ~1.2 microns with a PDI of ~0.7 for both the blank and PS-loaded particles (Table 1). SEM images of the particles can be seen in Fig. 1.

The zeta potential for the PS-loaded PLGA nanorods was −22 mV and −6.3 mV for the blank PLGA nanorods. The blank PLGA cylinder zeta potential was −32 mV whereas the PS-loaded PLGA cylinders had a zeta potential of −39 mV. The incorporation of PS significantly modified the negative charge of the resulting particles as a result of the anionic nature of the lipid. In addition, we evaluated the PS release kinetics in 1 × PBS using sink conditions and found that 90% of PS was released from the 80 × 320 nm PRINT particles by 4 h, while less than 15% of PS was released from the 1 micron cylinders by 4 h (Supplemental figure 1). Lastly, unadulterated, resuspended PS generated liposomes of 878 nm with a PDI of 1. This high PDI value indicates a broad size range of PS liposomes above and below the 878 nm average.

3.2. Particulate delivery of PS down-regulates the inflammatory response in dendritic cells

The innate immune response is critical in both triggering and resolving inflammatory responses as well as educating adaptive immune responses in large part via signaling through a number of pattern recognition receptor families and cytokine receptors [47,48]. As dendritic cells are key mediators of the innate immune response and serve a crucial role as antigen presenting cells in driving adaptive immune responses, we sought to address how geometric manipulation of PS could augment the immune response of dendritic cells (DC) to inflammatory stimuli. In particular, we evaluated the effect of PS-loaded PLGA nanorods on the inflammatory response in BMDCs stimulated with a Th1-like input (LPS/IFNγ) for 18 h. BMDCs treated with 80 × 320 nm PLGA nanorods encapsulating 25 μM of PS (PS Nanorod) showed a significant suppression of the IL-6 and IL-12 inflammatory response

compared to either 25 μM of liposomal PS (PS LIPO) or blank PLGA nanorods (BLK PRINT) (Fig. 2A). This cytokine suppression was consistent across a time range from 4 hrs to 18 hrs and was also found when assaying for the inflammatory mediators prostaglandin E2 and TNF-α (Supplemental figures 2 and 3).

Quantification of CD86 expression, an important DC receptor necessary for T cell stimulation, showed that PS nanorods inhibited DC maturation as evidenced by a near complete abrogation of CD86 upregulation in response to LPS/IFNγ. In contrast, liposomal PS and blank PLGA particles did not suppress CD86 upregulation (Fig. 2B). Interestingly, surface expression of MHC Class II molecules (I-Ab) and CD80 was not significantly downregulated by PS nanorods (data not shown). These data indicate PS is able to suppress the inflammatory response of DC while also impeding DC maturation cues in a manner that is dependent on the geometric presentation of PS.

3.3. Particulate delivery of PS downregulates myelin-specific T cell activation and cytokine responses

As our initial findings suggested DC could be skewed away from inflammatory responses in the presence of 80 × 320 nm PS-loaded PLGA nanorods, we next asked whether this immunomodulation of innate immune cells could be used to dampen an established effector T cell response. To evaluate the effectiveness of the PS-loaded PLGA particles in reducing T-cell activation and cytokine production, we made use of transgenic 2D2 mice. These transgenic mice have T cell receptors (TCRs) that are specific for myelin oligodendrocyte glycoprotein (MOG), a critical protein involved in the myelination of nerves in the central nervous system and one of the components that the body attacks in MS [49]. Because T cells of 2D2 mice process MOG in a Th1-biased manner, this experimental system enabled us to address whether delivery of PS may dampen an already established pro-inflammatory immune response to a known antigen.

2D2 T cells were incubated with DC that had been exposed to particles or controls in the presence and absence of MOG. As expected, in the absence of MOG there was little to no detectable IL-2, IL-6, TNFα, or IFNγ released (data not shown). However, when MOG was added to the system, a pro-inflammatory and T cell proliferative environment was triggered as evidenced by the robust production of IL-2, IL-6, TNFα, and IFNγ (Fig. 3A). In this type of mixed culture, T cells are the source of IFNγ and IL-2, while both T cells and DC produce TNFα and IL6. Liposomal PS could dampen production of these cytokines to variable degrees, but this effect required the highest PS dose used (50 μM). In contrast, particulate delivery of PS on 80 × 320 nm PLGA nanorods completely abolished IL-2 and IFNγ production and significantly reduced IL-6 and TNFα release to their baseline levels at the lowest PS dose used (12.5 μM) with only minimal enhancement seen when escalating the amount of PS delivered on nanorods.

Furthermore, as T regulatory cells (Tregs) are required for tolerance and dampening of effector T cell responses [50], we used flow cytometry to identify whether PS could augment the quantity of Tregs in our MOG assay. Twenty five micromolar PS-loaded 80 × 320 nm PLGA nanorods significantly increased the IL-10 and FOXP3 double-positive cell population that corresponds to T regulatory cells, whereas an equivalent dose of liposomal

PS did not cause an increase in the Treg population (Fig. 3B). It should be noted that the abrogation of IL-2 by PS nanorods will greatly reduce the proliferation of all T cell populations. Thus the overall number of Tregs may be unchanged but the relative number is heightened by PS nanorods due to the lack of effector T cell proliferation in comparison to the other treatment arms. As the balance between an effector response versus a tolerizing T regulatory response is dependent in part on the quantity of T cells, the relative abundance of effector versus Tregs and the cytokine milieu, it is plausible that particulate delivery of PS may help shift the balance towards tolerance through both reducing effector T cell proliferation and the amount of effector skewing cytokines [50,51]. These data clearly show that delivery of PS on a nanorod potently diminishes inflammatory cytokines and promotes Treg population abundance during an established effector T cell response that does not occur when an equivalent dose of PS is delivered on a liposome.

To further clarify whether this immune dampening effect was dependent on particle geometry, we fabricated 1 micron PLGA cylinders with PS and performed the same experiment (Fig. 3C). Interestingly, these 1 micron cylinders had an intermediate efficacy compared to liposomal PS and the 80 × 320 nm nanorods. For example, IL-2, IL-6 and TNFα release were diminished by 1 micron cylinder delivery of 12.5 μM PS, but to a significantly less level than for an equivalent dose of PS delivered by 80 × 320 nm nanorods. Conversely, liposomal PS was the least efficacious platform for all cytokines tested. At least four conclusions may be drawn from these findings: 1) There is a signaling threshold for the immune-suppressive effects of PS; 2) this threshold is achieved at much lower doses when PS is delivered via a PLGA nanorod particle; 3) the geometry of the particle itself may alter this threshold; and 4) the signaling pathways leading to production of individual cytokines may be differentially affected by particle geometry and ligand dose.

3.4. Suppression of autoimmune responses in vivo

Building on our previous findings, we next hypothesized that the 80 × 320 nm PS-loaded PLGA nanorods may be able to dampen autoimmune pathology. Multiple sclerosis is the most common autoimmune inflammatory demyelinating disease of the CNS. The pathogenesis of MS is driven by auto-reactive T cells and auto-antibodies creating multifocal areas of demyelination with loss of oligodendrocytes, astroglial scarring, and axonal injury [52,53]. It was recently discovered that myelin phospholipids are targeted by the autoimmune response in MS and that myelin phospholipids are natural anti-inflammatory class of compounds with the ability to suppress activation and inducing apoptosis of autoreactive T cells in MS [54–56]. Pertinently, PS was identified as one of the targeted myelin lipids and was among the most highly active in suppressing activation and inducing apoptosis of autoreactive T cells [56]. However, the ability to harness PS as a therapeutic component for MS has yet to be fully explored, possibly in part because of the ability of soluble PS to trigger clot formation [57].

To test whether particulate delivery of PS could ameliorate CNS disease, we used the experimental autoimmune encephalitis (EAE) model in C57BL/6 as it is the most common and well-characterized animal model of multiple sclerosis (MS) and has been used in the development of MS therapies [58]. Similar to MS patients, these mice suffer immune-cell

mediated lesions to white matter tracts of central nervous system tissue (CNS). The CNS tissue damage causes ascending limb paralysis which is evaluated by a standard clinical scoring system as described in the Methods section. Mice were intravenously treated with 50 μg of liposomal PS (PS LIPO), blank PLGA particles (BLK PRINT), or 50 μg of 80 × 320 nm PS-loaded PLGA nanorods (PS Nanorod) at times post-immunization as indicated by arrows in Fig. 4A. In addition, the disease incidence, day on onset, and maximum score of mice are shown in Fig. 4A and B. Mice treated with PS PRINT particles had a significantly lower burden of disease based on clinical scores and video evidence of reduced hind limb paralysis (Supplemental movie 1). Furthermore, the reduction in clinical severity was significantly more pronounced and occurred earlier after treatment in the group that received nanorod PS versus an equivalent dose of liposomal PS. These findings provide *in vivo* evidence for the use of particulate PS to ameliorate pathologic autoimmune responses with concomitant improvement in CNS function.

Supplementary data related to this article can be found online at http://dx.doi.org/10.1016/j.biomaterials.2015.08.040.

3.5. Suppression of allogenic human CD4$^+$ T cell activation via particulate delivery of PS

Given the above findings showing the capability for 80 × 320 nm nanorod delivery of PS to impede inflammatory innate immune responses and subsequent effector T cell proliferation, we hypothesized that this approach may be useful in abrogating the immune pathology caused by aberrant T cell activation in some human diseases. A proof of concept study using a mixed lymphocyte reaction to assess allogeneic human CD4$^+$ T cell activation was performed using healthy human blood donors. In this experiment, mixing T cells from one donor with DCs from another donor will trigger activation and proliferation of T cells as they recognize the DC as foreign due to MHC incompatibility [59].

While blank PLGA nanorods and liposomal PS similarly and modestly decreased proliferation of T cells from ~61% in the untreated group to ~50%, PS-loaded PLGA nanorods (PS Nanorod) significantly reduced T-cell activation and proliferation all the way to baseline levels of ~3% (Fig. 5A). This lack of T cell proliferation and activation was further evidenced by the significant reduction in IFNγ production seen only in the PS Nanorod group (Fig. 5B). These robust findings provide further evidence for the clear difference in biological signaling triggered by geometric manipulation of an equivalent dose of PS on a PLGA nanorod versus a liposome. That this work was carried out in primary human cells suggests that this may be a potential approach for reducing human T cell activation such as in transplant rejection and graft versus host disease.

4. Discussion

Given the exciting potential for nanomaterial-based biological programming, it is critical to elucidate how particulate presentation of ligands may affect subsequent signaling from cognate receptors. Our aim in this report was to determine whether particulate presentation of a model cell surface receptor ligand, phosphatidylserine, would augment downstream signaling effects and whether this could be used for therapeutic benefit. We made use of the PRINT fabrication process which exquisitely controls particle, size, shape and composition.

This enabled us to directly compare biological responses to equivalent doses of PS delivered in liposomal or PLGA particle fashion. By adjusting particle size and shape, we could further tease out whether the geometry of PS presentation itself can tune signaling events. While previous studies have looked at liposomal formulations of PS, none to our knowledge have directly compared the signaling efficacy of liposomal PS versus PS-loaded PLGA particles on immune responses nor controlled as we have for particle geometry [33–35]. Through our studies, we identified a clear and significant enhancement of the anti-inflammatory and T cell dampening effects of PS by manipulation of its geometric presentation to innate immune cells that may be of therapeutic benefit in a variety of disease contexts.

Our studies consistently found that for an equivalent dose of PS, its presentation on an 80 × 320 nm PLGA nanorod was significantly more efficacious than a liposomal or 1 micron PLGA cylinder formulation. This may indicate geometric manipulation of PS confers emergent properties upon the ligand through augmenting its interactions with its cell surface receptors. Such a finding would be in line with a large body of evidence addressing cellular signaling pathways downstream of cell surface receptors. For example, the fungal cell wall moiety beta-glucan requires particulate presentation in order to trigger signaling through its cognate pattern recognition receptor Dectin-1 [60]. The particulate presentation of beta-glucan enables formation of a phagocytic synapse through receptor clustering of Dectin-1 only in the presence of intact fungi. Elegantly, this mechanism enables innate immune cells to trigger anti-fungal responses only when they encounter an intact fungus as opposed to simply a soluble component of the fungal cell wall.

As inflammation drives both innate immune and effector T cell responses but also tissue pathology, finding means of countering inflammatory programs in situ would be of great benefit [48]. While standard clinical options for excessive inflammation or undesired immune responses include systemic immunosuppression or systemic blockade of cytokines, more targeted and transient solutions are sorely needed. Our studies addressing the potential for PS particles to dampen effector immune responses using the 2D2 transgenic T cells, an *in vivo* model of multiple sclerosis, and an assay of organ rejection provide strong evidence that geometric manipulation of PS may be an attractive modality for quenching pathologic inflammatory responses and undesired effector T cell proliferation to promote Treg abundance.

Our studies suggest PS particles themselves drive an anti-inflammatory program that is antigen-independent, which may explain why the clinical improvement in the EAE model was limited to a short window after dosing with PS stopped. Two recent papers from the Miller group showed a transient efficacy in the EAE model when using a nanoparticle platform that depleted inflammatory cells whereas an antigen-dependent nanoparticle approach did not require continued dosing for efficacy [19,23]. Further studies are underway to address whether PS particles co-delivering an antigen could drive antigen-specific immune tolerance. Regardless, the potential therapeutic use of biomaterials to program tolerance in the setting of autoimmunity and transplantation could fundamentally improve the clinical outcomes for millions of patients [25,61].

5. Conclusions

We show that particulate presentation of PS on 80 × 320 nm PLGA nanorods enhances its signaling efficacy to dampen inflammation and promote immune tolerance through inhibiting effector T cell expansion while maintaining T regulatory cells. These effects are dependent on the geometry of PS presentation as PS liposomes and PS delivered on a 1 micron PLGA cylinder are less efficacious for a given PS dose than 80 × 320 nm nanorods. Geometric manipulation of PS was used therapeutically to reduce disease in a model of multiple sclerosis and also to block effector T cell responses in primary human immune cells in an allogenic mixed lymphocyte reaction. These results not only identify a promising therapeutic strategy for a variety of immune-related conditions but also give evidence for manipulation of ligand geometry via biomaterials as a means to tailor programming of cellular signaling networks. The ability to tune the kinetics and magnitude of cellular signaling may afford unforeseen advantages in future therapeutics given these features are critical to encoding cellular function [62].

Supplementary Material

Refer to Web version on PubMed Central for supplementary material.

Acknowledgments

We would like to thank the UNC Animal Studies Core for their contributions to this work. This work was funded in part by NC TRACS 100K1202, MS society grant CA1068-A-10 and NIH U19AI109784 (JPT and JMD); UCRF UNC Internal Grants (JPT); and NIH 8-VP1-CA174425-04 (JMD). TKE was supported by a fellowship from the Cancer Research Institute; JDB was supported by a National Defense Science and Engineering Graduate Fellowship and PhRMA Foundation Fellowship; RAR was supported by NIH training grant T32-AI007273-25 and the University Cancer Research Fund. JDB and RAR were also supported by the UNC Medical Scientists Training Program NIGMS-2-T32-GM008719. Conflicts of interest: Joseph M. DeSimone is a founder and maintains a financial interest in Liquidia Technologies. PRINT and Fluorocur are registered trademarks of Liquidia Technologies, Inc. The University of North Carolina has filed a patent application related to this work (PCT/US2014/064312).

References

1. Irvine DJ, Swartz MA, Szeto GL. Engineering synthetic vaccines using cues from natural immunity. Nat. Mater. 2013; 12:978. 11//print. [PubMed: 24150416]
2. Moon JJ, Huang B, Irvine DJ. Engineering nano- and microparticles to tune immunity. Adv. Mater. Jul 24.2012 24:3724. [PubMed: 22641380]
3. Hubbell JA, Thomas SN, Swartz MA. Materials engineering for immuno-modulation. Nature. Nov 26.2009 462:449. [PubMed: 19940915]
4. Swartz MA, Hirosue S, Hubbell JA. Engineering approaches to immuno-therapy. Sci. Transl. Med. Aug 22.2012 4:148rv9.
5. Kim J, et al. Injectable, spontaneously assembling, inorganic scaffolds modulate immune cells in vivo and increase vaccine efficacy. Nat. Biotech. 2015; 33:64. 01//print.
6. Li AV, et al. Generation of effector memory T cellebased mucosal and systemic immunity with pulmonary nanoparticle vaccination. Sci. Transl. Med. Sep 25.2013 5:204ra130.
7. Moon JJ, et al. Interbilayer-crosslinked multilamellar vesicles as synthetic vaccines for potent humoral and cellular immune responses. Nat. Mater. Mar.2011 10:243. [PubMed: 21336265]
8. Demento SL, et al. Inflammasome-activating nanoparticles as modular systems for optimizing vaccine efficacy. Vaccine. May 18.2009 27:3013. [PubMed: 19428913]

9. Eggermont LJ, Paulis LE, Tel J, Figdor CG. Towards efficient cancer immunotherapy: advances in developing artificial antigen-presenting cells. Trends Biotechnol. Sep; 2014 32(9):456–465. [PubMed: 24998519]
10. Park J, et al. Combination delivery of TGF-beta inhibitor and IL-2 by nanoscale liposomal polymeric gels enhances tumour immunotherapy. Nat. Mater. Oct.2012 11:895. [PubMed: 22797827]
11. Chauhan VP, Jain RK. Strategies for advancing cancer nanomedicine. Nat. Mater. 2013; 12:958. 11//print. [PubMed: 24150413]
12. Chow EK-H, Ho D. Cancer nanomedicine: from drug delivery to imaging. Sci. Transl. Med. Dec 18.2013 5:216rv4.
13. Jain RK, Stylianopoulos T. Delivering nanomedicine to solid tumors. Nat. Rev. Clin. Oncol. Nov. 2010 7:653. [PubMed: 20838415]
14. Sheen MR, Lizotte PH, Toraya-Brown S, Fiering S. Stimulating antitumor immunity with nanoparticles. Wiley Interdiscip. Rev. Sep.2014 6:496.
15. von Maltzahn G, et al. Nanoparticles that communicate in vivo to amplify tumour targeting. Nat. Mater. Jul.2011 10:545. [PubMed: 21685903]
16. Wang AZ, Langer R, Farokhzad OC. Nanoparticle delivery of cancer drugs. Annu. Rev. Med. 2012; 63:185. [PubMed: 21888516]
17. Ali OA, Emerich D, Dranoff G, Mooney DJ. In situ regulation of DC subsets and T cells mediates tumor regression in mice. Sci. Transl. Med. Nov 25.2009 1:8ra19.
18. Ali OA, et al. Identification of immune factors regulating anti-tumor immunity using polymeric vaccines with multiple adjuvants. Cancer Res. Mar 15; 2014 74(6):1670–1681. [PubMed: 24480625]
19. Getts DR, et al. Therapeutic inflammatory monocyte modulation using immune-modifying microparticles. Sci. Transl. Med. Jan 15.2014 6:219ra7.
20. Fredman G, et al. Targeted nanoparticles containing the proresolving peptide Ac2-26 protect against advanced atherosclerosis in hypercholesterolemic mice. Sci. Transl. Med. Feb 18.2015 7:275ra20.
21. Gadde S, et al. Development of therapeutic polymeric nanoparticles for the resolution of inflammation. Adv. Healthc. Mater. Sep; 2014 3(9):1448–1456. [PubMed: 24659608]
22. Kamaly N, et al. Development and in vivo efficacy of targeted polymeric inflammation-resolving nanoparticles. Proc. Natl. Acad. Sci. U. S. A. Apr 16.2013 110:6506. [PubMed: 23533277]
23. Getts DR, et al. Microparticles bearing encephalitogenic peptides induce T-cell tolerance and ameliorate experimental autoimmune encephalomyelitis. Nat. Biotechnol. Dec.2012 30:1217. [PubMed: 23159881]
24. Hunter Z, et al. A biodegradable nanoparticle platform for the induction of antigen-specific immune tolerance for treatment of autoimmune disease. ACS Nano. Mar 25; 2014 8(3):2148–2160. [PubMed: 24559284]
25. Maldonado RA, et al. Polymeric synthetic nanoparticles for the induction of antigen-specific immunological tolerance. Proc. Natl. Acad. Sci. U. S. A. Jan 13.2015 112:E156. [PubMed: 25548186]
26. Moraga I, et al. Tuning cytokine receptor signaling by re-orienting dimer geometry with surrogate ligands. Cell. Mar 12.2015 160:1196. [PubMed: 25728669]
27. Henson PM, Bratton DL. Antiinflammatory effects of apoptotic cells. J. Clin. Investig. Jul.2013 123:2773. [PubMed: 23863635]
28. Huynh ML, Fadok VA, Henson PM. Phosphatidylserine-dependent ingestion of apoptotic cells promotes TGF-beta1 secretion and the resolution of inflammation. J. Clin. Investig. Jan.2002 109:41. [PubMed: 11781349]
29. Hochreiter-Hufford A, Ravichandran KS. Clearing the dead: apoptotic cell sensing, recognition, engulfment, and digestion. Cold Spring Harb. Perspec. Biol. Jan 1.2013 5
30. Graham DK, DeRyckere D, Davies KD, Earp HS. The TAM family: phosphatidylserine sensing receptor tyrosine kinases gone awry in cancer. Nat. Rev. Cancer. Dec.2014 14:769. [PubMed: 25568918]

31. Frey B, Gaipl US. The immune functions of phosphatidylserine in membranes of dying cells and microvesicles. Semin. Immunopathol. Sep.2011 33:497. [PubMed: 20941495]
32. Yang H, et al. A lysine-rich motif in the phosphatidylserine receptorPSR-1 mediates recognition and removal of apoptotic cells. Nat. Commun. 2015; 6 01/07/online.
33. Chen X, Doffek K, Sugg SL, Shilyansky J. Phosphatidylserine regulates the maturation of human dendritic cells. J. Immunol. Sep 1.2004 173:2985. [PubMed: 15322157]
34. Harel-Adar T, et al. Modulation of cardiac macrophages by phosphatidylserine-presenting liposomes improves infarct repair. Proc. Natl. Acad. Sci. U. S. A. Feb 1.2011 108:1827. [PubMed: 21245355]
35. Ramos GC, et al. Apoptotic mimicry: phosphatidylserine liposomes reduce inflammation through activation of peroxisome proliferator-activated receptors (PPARs) in vivo. Br. J. Pharmacol. 2007; 151:844. [PubMed: 17533418]
36. Canelas DA, Herlihy KP, DeSimone JM. Top-down particle fabrication: control of size and shape for diagnostic imaging and drug delivery. Wiley Interdiscip. Rev. Jul.2009 1:391.
37. Gratton SE, et al. The pursuit of a scalable nanofabrication platform for use in material and life science applications. Acc. Chem. Res. Dec.2008 41:1685. [PubMed: 18720952]
38. Perry JL, Herlihy KP, Napier ME, Desimone JM. PRINT: a novel platform toward shape and size specific nanoparticle theranostics. Acc. Chem. Res. Oct 18.2011 44:990. [PubMed: 21809808]
39. Rolland JP, et al. Direct fabrication and harvesting of monodisperse, shape-specific nanobiomaterials. J. Am. Chem. Soc. Jul 20.2005 127:10096. [PubMed: 16011375]
40. Roberts RA, et al. Analysis of the murine immune response to pulmonary delivery of precisely fabricated nano- and microscale particles. PLoS One. 2013; 8:e62115. [PubMed: 23593509]
41. Robbins GR, et al. Analysis of human innate immune responses to PRINT fabricated nanoparticles with cross validation using a humanized mouse model. Nanomed. Nanotechnol. Biol. Med. Apr. 2015 11:589.
42. Jones SW, et al. Nanoparticle clearance is governed by Th1/Th2 immunity and strain background. J. Clin. Investig. Jul.2013 123:3061. [PubMed: 23778144]
43. Fromen CA, et al. Controlled analysis of nanoparticle charge on mucosal and systemic antibody responses following pulmonary immunization. Proc. Natl. Acad. Sci. U. S. A. Jan 13.2015 112:488. [PubMed: 25548169]
44. Schneider M, et al. The innate immune sensor NLRC3 attenuates toll-like receptor signaling via modification of the signaling adaptor TRAF6 and transcription factor NF-kappaB. Nat. Immunol. Sep.2012 13:823. [PubMed: 22863753]
45. Eitas TK, et al. The nucleotide-binding leucine-rich repeat (NLR) family member NLRX1 mediates protection against experimental autoimmune encephalomyelitis and represses macrophage/microglia-induced inflammation. J. Biol. Chem. Feb 14.2014 289:4173. [PubMed: 24366868]
46. Miller SD, Karpus WJ. John, E. ColiganExperimental autoimmune encephalomyelitis in the mouse. Current Protocols in Immunology. May.2007 (Chapter 15), Unit 15 1.
47. Blander JM, Medzhitov R. On regulation of phagosome maturation and antigen presentation. Nat. Immunol. Oct.2006 7:1029. [PubMed: 16985500]
48. Medzhitov R. Origin and physiological roles of inflammation. Nature. Jul 24.2008 454:428. [PubMed: 18650913]
49. Bettelli E. Building different mouse models for human MS. Ann. N. Y. Acad. Sci. Apr.2007 1103:11. [PubMed: 17376825]
50. Wing K, Sakaguchi S. Regulatory T cells exert checks and balances on self tolerance and autoimmunity. Nat. Immunol. 2010; 11:7. 01//print. [PubMed: 20016504]
51. Steinman RM, Hawiger D, Nussenzweig MC. Tolerogenic dendritic cells. Annu. Rev. Immunol. 2003; 21:685. [PubMed: 12615891]
52. McFarland HF, Martin R. Multiple sclerosis: a complicated picture of auto-immunity. Nat. Immunol. Sep.2007 8:913. [PubMed: 17712344]

53. Schirmer L, Antel JP, Bruck W, Stadelmann C. Axonal loss and neurofilament phosphorylation changes accompany lesion development and clinical progression in multiple sclerosis. Brain Pathol. Jul.2011 21:428. [PubMed: 21114565]
54. Genain CP, Cannella B, Hauser SL, Raine CS. Identification of autoantibodies associated with myelin damage in multiple sclerosis. Nat. Med. Feb.1999 5:170. [PubMed: 9930864]
55. Goverman J. Autoimmune T cell responses in the central nervous system. Nat. Rev. Immunol. Jun. 2009 9:393. [PubMed: 19444307]
56. Ho PP, et al. Identification of naturally occurring fatty acids of the myelin sheath that resolve neuroinflammation. Sci. Transl. Med. Jun 6.2012 4:137ra73.
57. Majumder R, Weinreb G, Zhai X, Lentz BR. Soluble phosphatidylserine triggers assembly in solution of a prothrombin-activating complex in the absence of a membrane surface. J. Biol. Chem. Aug 16.2002 277:29765. [PubMed: 12045194]
58. Rangachari M, Kuchroo VK. Using EAE to better understand principles of immune function and autoimmune pathology. J. Autoimmun. Sep.2013 45:31. [PubMed: 23849779]
59. Levitsky J, et al. The human “Treg MLR”: immune monitoring for FOXP3+ T regulatory cell generation. Transplantation. Dec 15.2009 88:1303. [PubMed: 19996930]
60. Goodridge HS, et al. Activation of the innate immune receptor dectin-1 upon formation of a ‘phagocytic synapse’. Nature. Apr 28.2011 472:471. [PubMed: 21525931]
61. Zakrzewski JL, van den Brink MRM, Hubbell JA. Overcoming immunological barriers in regenerative medicine. Nat. Biotech. 2014; 32:786. 08//print.
62. Jeremy E, Purvis G. Lahav. Encoding and decoding cellular information through signaling dynamics. Cell. 2013; 152:945. [PubMed: 23452846]

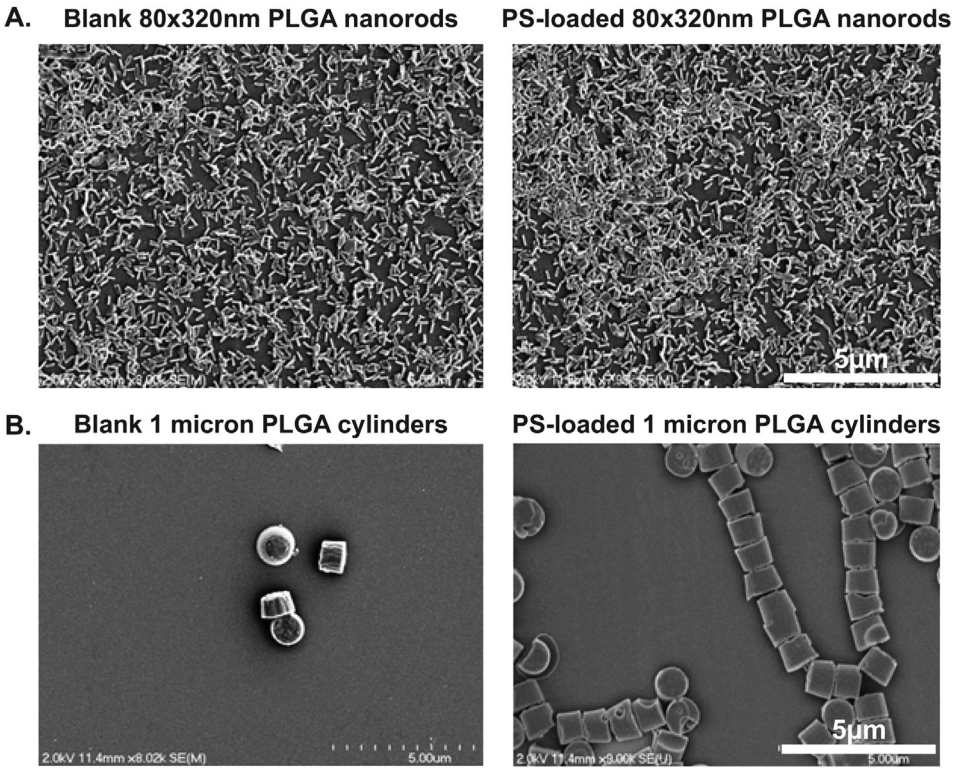

Fig. 1.

SEM images of PRINT particles. A. Blank and PS-loaded 80 × 320 nm nanorods. B. Blank and PS-loaded 1 micron cylinders.

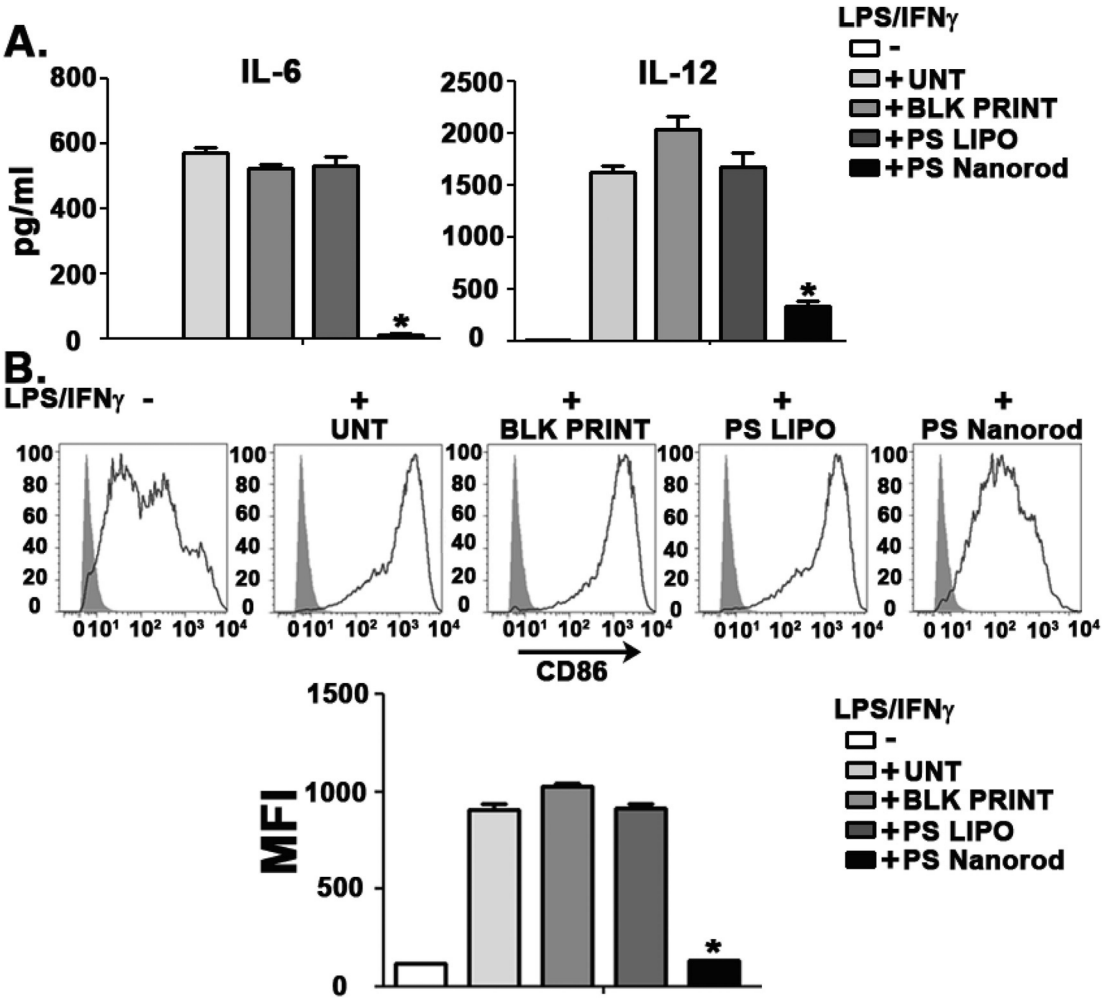

Fig. 2.

PS nanorods downregulate inflammatory responses in dendritic cells. A. ELISA analysis of IL-6 (left) and IL-12(p40) (right) in DC cultures stimulated with LPS(10 ng/ml) and IFNγ(10 ng/ml) for 18 h. PS was dosed at 25 μM in either liposomal (PS LIPO) or 80 × 20 nm nanorod formulation (PS Nanorod). Blank 80 × 320 nm PLGA particles (BLK PRINT) were used as a negative control. B. Flow cytometry-based histogram analysis of surface expression of CD86. Cells were initially gated as $CD11c^{+}$. MFI represents Mean Fluorescent Intensity. Results are representative of three independent experiments. Error bars represent ± s.e.m. * = $P < .0001$.

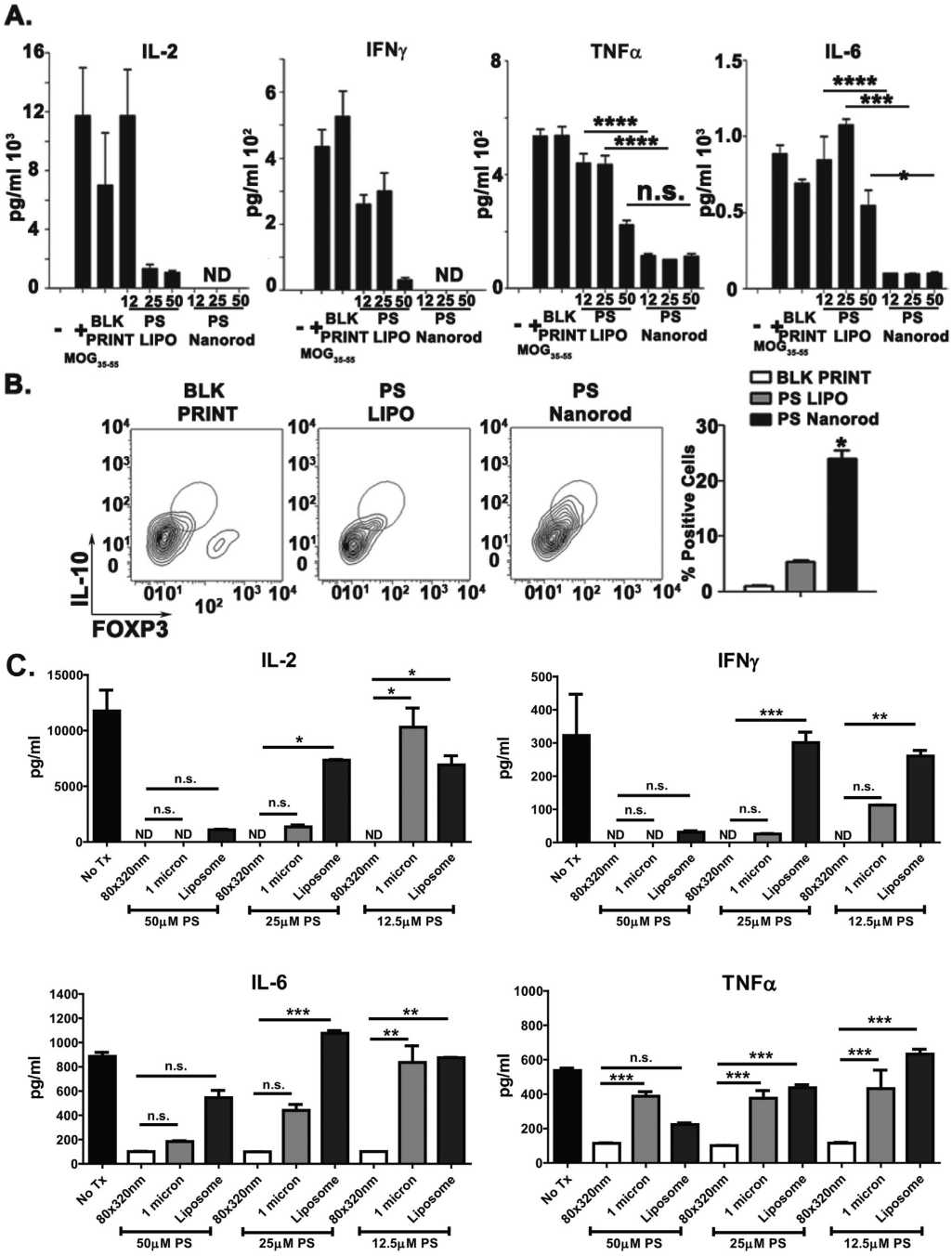

Fig. 3.

Geometric manipulation of PS downregulates myelin-specific T cell activation and cytokine responses. A. ELISA analysis of 2D2 Tg $CD4^+$ T cells activated with $MOG_{35–55}$-pulsed DCs. Supernatants were collected 48 hpi. PS doses ranged from 12.5 to 50 μM in either liposomal (PS LIPO) or 80 × 20 nm nanorod formulation (PS Nanorod). B. Left, contour plot depicting intracellular flow cytometry-based of IL-10^+, $FoxP3^+$ population. Right, quantification of IL-10^+, $FoxP3^+$ cell population. Cells were initially gated as $CD3^+$. C. ELISA analysis of 2D2 Tg $CD4^+$ T cells activated with $MOG_{35–55}$-pulsed DCs.

Supernatants were collected 48 hpi. PS doses ranged from 12.5 to 50 μM in liposomal, 80 × 320 nm PLGA nanorod or 1 μm PLGA cylinder formulations. Results are representative of three independent experiments. Error bars represent ± s.e.m. * = $P < .05$; ** = $P < .01$; *** = $P < .001$; *** = $P < .0001$.

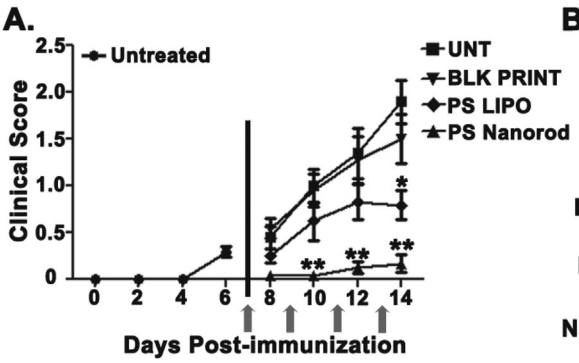

B.

	Disease Incidence	Maximum Score
UNT	100%(10/10)	1.9 (+/- 0.2)
BLK PRINT	100%(11/11)	1.5 (+/- 0.3)
PS LIPO	83% (10/12)	0.8 (+/- 0.2)
PS Nanorod	25% (3/12)	0.2 (+/- 0.1)

Fig. 4.

PS Nanorods suppress autoimmune responses *in vivo*. A. Clinical scores of mice treated as indicated. Scores represent the combination of two independent experiments of 5–6 mice per group. Mice were intravenously treated with 50 μg of liposomal PS (PS LIPO), 50 μg of PS on 80 × 320 nm PLGA nanorods (PS Nanorod), or an equivalent dose of Blank PLGA particles (BLK PRINT) at times indicated by arrows. B. Table depicting disease incidence, day on onset, and maximum score of mice depicted in panel A.

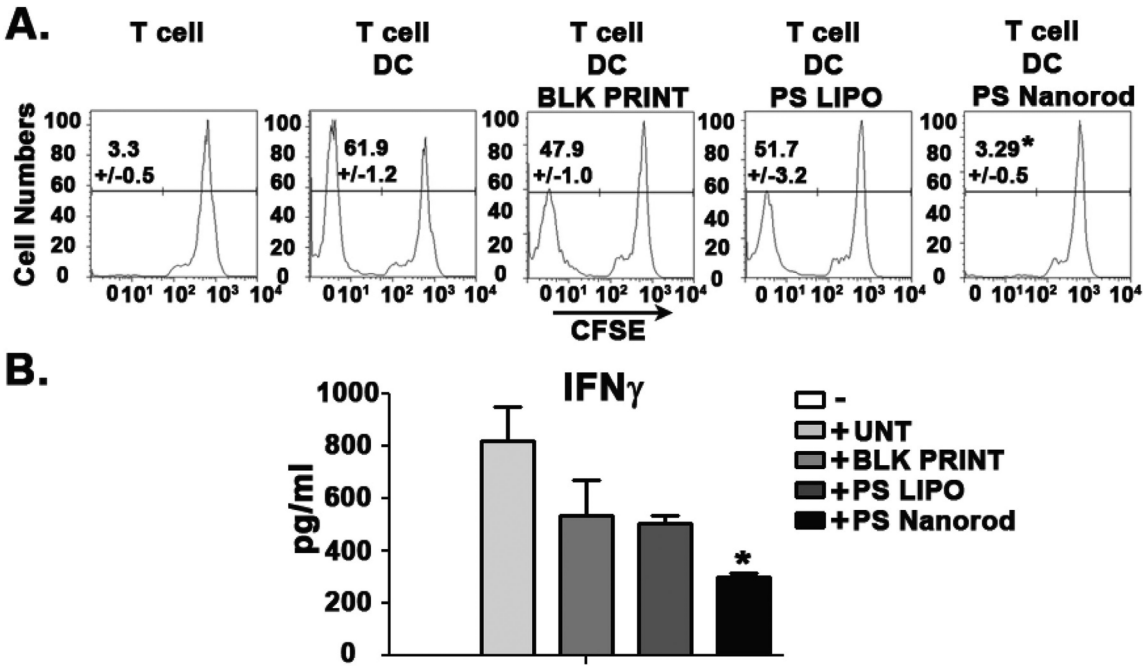

Fig. 5.

PS Nanorods are efficacious in reducing the activation of human immune cells. A. CFSE dilution analysis of allogenic human $CD4^+$ T cell activation 7 days post activation. B. ELISA analysis of allogenic $CD4^+$ T cell activation. Supernatants were collected 7 days post activation. Results are representative of two independent experiments with four $CD4^+$ T cell donors and two DC donors. Cells were initially gated as $CD3^+$. Error bars represent ± s.e.m. * = $P < .05$.

Table 1

PRINT particle characteristics.

Formulation	Size (nm)	PDI	Zeta potential (mV)	Weight % PS
80 × 320 nm Blank PLGA nanorod	208.3 ± 3.0	0.104	–6.3 ± 1.001	0
80 × 320 nm PS PLGA nanorod	209.1 ± 3.1	0.048	–22.0 ± 2.423	8.0 ± 2.1
1 μm Blank PLGA cylinder	1202 ± 31.1	0.684	–31.8 ± 0.173	0
1 μm PS PLGA cylinder	1272 ± 35.8	0.714	–39.4 ± 0.651	11.2 ± 3.0.2